Multielectron X-Ray Photoexcitation Measurements in Krypton

Moshe Deutsch
Physics Department, Bar-Ilan University, Ramat-Gan, Israel
and
Michael Hart
Schuster Laboratory, University of Manchester, Manchester M13 9PL, United Kingdom
(Received 11 June 1986)

X-ray photoabsorption measurements were carried out on krypton near the $1s$ ionization threshold, by use of synchrotron radiation. A rich, well resolved spectrum of simultaneous two- and three-electron excitations is detected. Feature identification is supported by both relativistic and nonrelativistic calculations. The data support in detail the $Z+1$ approximation for both two- and three-electron excitations. No indication of a preferred Coster-Kronig decay channel for $1s4s$ hole states is found, in contrast with argon. The partial cross sections are in good accord with shakeup theory and photoelectron data on other noble gases.

PACS numbers: 32.30.Rj, 32.80.Fb, 78.70.Dm

Multielelctron processes epitomize the breakdown of the single-electron–fixed-potential models and provide, *in potentia,* a basis for understanding electron-electron correlation and the excitation dynamics in atoms.[1] X-ray absorption spectroscopy is a well established method for the direct probing of electronic energy levels and interaction cross sections in atoms and, thus, a method of choice for multielectron excitation studies. However, as the cross sections involved are very small, only a few absorption studies on noble gases,[2,3] transition metals,[4] and several mid-Z elements[5] have been published. All but one of these were of low resolution and features due to the numerous bound-bound and bound-free multielectron transitions were not observed. The recent synchrotron study of Ar by Deslattes *et al.*[3] is the only one where several sharp features associated with two-electron $[1s3p]$ excitations and the lowest-lying $[1s3s]$ one were resolved. (Square brackets indicate vacant orbitals throughout this paper.)

We report here high-resolution photoabsorption measurements in the K-edge region of Kr. Both $[1s4p]$ and $[1s4s]$ two-electron and $[1s4p^2]$ three-electron features were clearly resolved and identified. Relativistic Dirac-Fock (RDF)[6] and nonrelativistic Hartree-Fock (HF)[7] energy levels agree well with the data, as do those derived from Rb optical data in the $Z+1$ approximation.

The measurements were carried out at the Daresbury Laboratory Synchrotron Radiation Source, United Kingdom, running at 2 GeV and 110 mA. The Kr sample, of 99.995+% purity, was contained at a pressure of 750 mm Hg (25 °C) in a sealed cell 30 mm long having beryllium windows. Its temperature was continuously monitored and changed less than 0.5 °C throughout a complete scan. Sealed argon-ionization-chamber detectors were used to measure the incident and transmitted intensities. A monolithic two-reflection silicon 220 monochromator was employed, yielding an effective energy resolution $\lesssim 1$ eV. Total harmonic contamination was below 0.5% and varied smoothly with energy. Repeated scanning allowed the elimination of spurious intensity changes. An absolute energy scale was established by employment of published Kr K and Bi L_{I} edge data.[8] Further details can be found elsewhere.[9]

The measured K edge is shown in Fig. 1 versus the energy shift from the onset of the one-electron continuum[8] $E[1s]=14\,327.17$ eV. As only local abrupt in-

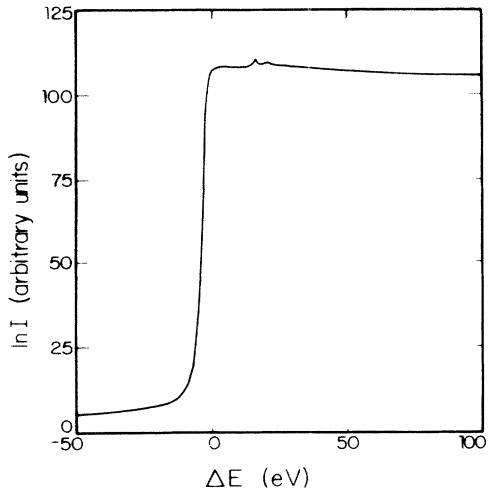

FIG. 1. Measured transmission spectrum of Kr. The energy is relative to the onset of the $[1s]$ continuum at 14 327.17 eV. Note the multielectron features near -20 eV.

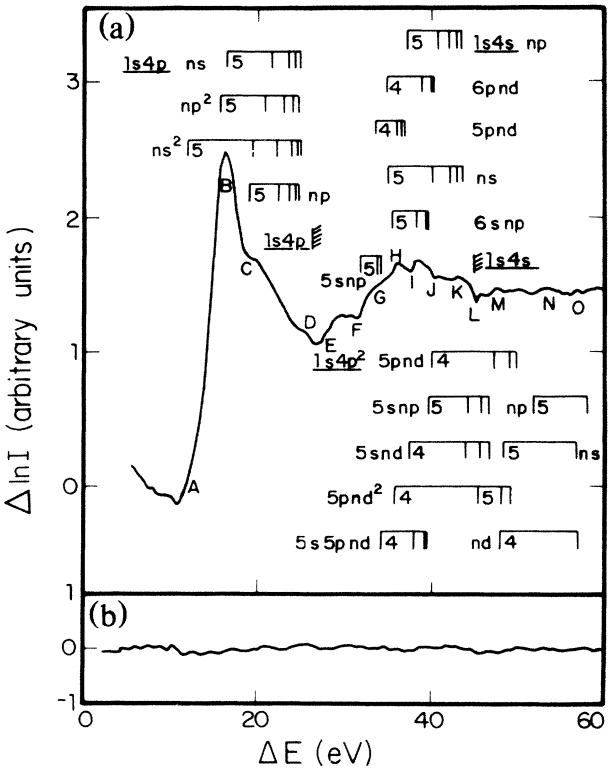

FIG. 2. (a) Expanded view of the multielectron features, and corresponding theoretical energy levels. (b) No-sample scan. Note the low level of noise. Both curves are difference plots. For details see text. (In this figure, underlining indicates vacant orbitals.)

tensity changes are of interest the transmitted intensity I was not normalized to the incident intensity I_0, thus eliminating a significant source of experimental noise. The multielectron features are clearly seen near ~ 20 eV.[10] A finer scan of these features is given in Fig. 2(a) as a plot of the difference between values of $\ln I$ and a straight line fitted to them just above the K edge. Figure 2(b) is an identically treated no-sample scan showing the noise level. The figure also shows the energy levels, calculated by use of RDF[6] and HF[7] methods. Most of these are also listed in Table I along with levels obtained from Rb optical data[11-13] in the $Z+1$ approximation. The RDF and HF methods were found to yield equal results to within ≤ 0.1 eV. The optical data agree with the HF calculations to better than 1 eV, with very few exceptions. This, and similar results obtained for Ar,[3] lend additional and detailed support for the validity of the $Z+1$ approximation.

The very small shoulder marked A in Fig. 2(a) and the preceeding dip are mainly associated with the $[1s4p]5s^2$ state with a possible smaller contribution from the $[1s4p]5s4d$ configuration, and the peak B—mainly with $[1s4p]5p^2$. The intensity ratio of these features reflects the much lower probability for a conjugate shakeup (CSU) process as compared to a shakeup (SU) one.[14] The step-shaped feature C marks the onset of $[1s4p]5p$, the lowest single-ion state populated by a SU process. The CSU $[1s4p]4d$ and $[1s4p]6s^2$ configurations may also contribute. The onset of the first double-ion state, $[1s4p]$, is responsible for the steplike feature E, while the weak shoulder D is in good alignment with the closely spaced, higher-order members of the single-ion series $[1s4p]np$ and the neutral configuration series $[1s4p]np^2$.

The opening of the $[1s4s]$ channel by $[1s4s]5s5p$ is marked by the Fano-shaped resonance E,F,G, slightly distorted by the fast increasing $[1s4p]$ background. The corresponding feature in Ar also has a Fano shape, characteristic of interference between quasibound levels and degenerate continua.[3] G is well aligned with the high-order members of the SU series $[1s4s]5snp$ as well as the lowest three-electron configuration $[1s4p^2]5s5p4d$. Another Fano-shaped resonance marks the onset of the first SU-populated single-ion configuration $[1s4s]5s$ at H,I, with possible contributions from the neutral SU states $[1s4s]6s5p$ and $[1s4s]6s6p$, respectively. The weak window J could be associated with the single-ion configuration $[1s4s]6s$ as well as several other CSU two-electron configurations. The Fano-shaped resonance K,L is clearly associated with the double-ion configuration $[1s4s]$, with possible contributions from the three-electron configuration $[1s4p^2]5p5d^2$.

The abundance of sharp features found here to be associated with the various $[1s4s]$ excitations is in marked contrast with the complete absence of corresponding features in the Ar measurements of Deslattes *et al.*[3] This was assumed to result from a greatly enhanced probability for neutral $[1s3s]$ states to undergo a fast Coster-Kronig (CK) transition to $[1s3p]$ states, relative to that to $[1s3p]$ states. Our data do not support a similar conclusion for Kr. This difference, if not an artifact, could reflect some basic difference in the binding strength of the outer electrons of the two atoms. Energy-dependent emission intensity measurements of the $k\beta^{11}$ satellite of Kr which could clarify this point are not available at the present.

Only three-electron (or higher) features are possible beyond the $[1s4s]$ double-ion edge. Thus, the three features M, N, and O, which though very weak show up above the noise level in all data sets measured, are clearly associated with three-electron configurations. M is in good alignment with $[1s4p^2]5p5d$ as well as $[1s4p^2]4d$ and $[1s4p^2]5s$, with angular-momentum–change considerations favoring the first of these. N is clearly associated with the double-ion configuration $[1s4p^2]5p$ and O, which seems to have, again, a Fano shape, is well aligned with the three double-ion configurations: $[1s4p^2]6s$, $[1s4p^2]5d$, and $[1s4p^2]6p$.

TABLE I. Energy levels obtained from RDF and HF calculations and optical Rb data in the $Z+1$ approximation. All energies in electronvolts.

Kr Configuration		Hf and RDF ΔE	Rb Configuration	z+1 Approximation[c] Range	Average
[1s]		0	$4p^6$	0	0
[1s4p]	$5s^2$	12.25	[4p]$5s^2$	11.13-11.98	11.56
	5s4d	14.15	5s4d	13.03-15.03	14.18
	5s5d	15.78	5s5d	14.95-16.41	15.75
	$5p^2$	16.06			
	$4d^2$	16.60			
	5s	16.87	5s	16.53-17.79	16.94
	4d	18.78	4d	17.73-21.04[a]	18.72
	5p	19.32	5p	19.13-20.78	19.93
	$6s^2$	19.86			
	$6p^2$	21.23			
	6p	22.86			
	$7p^2$	23.40			
	7p	23.95			
[1s4p]		26.67	[4p]		27.51
[1s4s]	5s5p	32.11			
	5p4d	34.02			
	5s6p	34.02			
	5s7p	34.56			
	5s	35.38			
	6s5p	35.92			
	4d	36.74			
	5p	37.82			
	6s6p	38.64			
	6s	40.55			
[1s4s]		45.17	[4s]		43.63[b]
[1s4p^2]	5s5p4d	34.29			
	5p5d^2	45.44			
	5p5d	47.35			
	4d	47.89	[$4p^2$]4d	46.69-54.12[b]	49.41
	5s	48.44	5s	48.23-52.82[b]	49.96
	5p	51.97	5p	52.08-57.21[b]	53.57
	5d	56.87	5d	57.62-59.68[c]	58.33
	6s	56.89			
	6p	58.23			
[1s4p^2]		65.85	[$4p^2$]		67.19

[a]Reference 12.
[b]Reference 13.
[c]Reference 14.

Currently available theoretical calculations, such as HF and RDF, are based on the independent-particle model and are, therefore, insufficient for a detailed understanding of multielectron excitations where many-body effects play an important role.[5,15] Moreover, even the energy dependence of the $[1s]$ cross section near threshold is not yet fully understood. The important role of post collisional interactions, for example, is just starting to emerge.[9,16] We feel, therefore, that a detailed cross-section modeling of our data is, at this stage, premature. To gain some insight, however, we adopt the somewhat arbitrary approximation[4,5] $\sigma = -\ln(I/I')$, where I and I' are the intensities just above and below the edge in question, respectively. For B in Fig. 2(a) we obtain $\sigma_B/\sigma_{[1s]} \approx 2.2 \times 10^{-2}$, slightly smaller than 3.4×10^{-2} which we deduced for the corresponding feature in the Ar data.[3] From C we obtain $\sigma_{[1s4p]5p}/\sigma_{[1s]} \approx 2.8\times10^{-3}$. Now, if the increase from E to H is attributed mainly to $[1s4p]$ then $\sigma_{[1s4p]}/\sigma_{[1s4p]5p} \approx 2.2$ is close to

$\sigma_{(\epsilon,\epsilon)}/\sigma_{(\epsilon,n)} \approx 2$ obtained for KL double excitations in Ne from photoelectron data.[17] Extrapolating the average level in the I,J,K region to beyond the $[1s4s]$ series limit yields $\sigma_{[1s4s]}/\sigma_{[1s]} \approx 2\times10^{-3}$. This and the $\sigma_{[1s4p]}$ value indicate an equal angular-momentum–independent probability *per electron* for $[1s4l]$ double ionization, in full accordance with shakeup theory.[15,18] Finally, the three-electron features M, N, and O yield $\sigma/\sigma_{[1s]} \approx 6\times10^{-4}$, 5×10^{-4}, and 4×10^{-4}, respectively, in good agreement with the value of 8×10^{-4} measured[4] for $[1s2p3p]$ and $[1s2s3p]$ in Ni.

We presented here a detailed high-resolution spectrum of the K-edge region of Kr where two- and three-electron features were resolved for the first time. While the energy levels observed are in good agreement with theory, a detailed modeling of the data will have to await the advent of a unified theory of electron excitation,[15] including both single and multielectron effects. Additional high-resolution data of the kind presented here, in particular for Ne, Xe, and Rn, should prove invaluable in achieving this goal.

One of us (M.D.) gratefully acknowledges a Science and Engineering Research Council senior visiting fellowship, as well as several important discussions with H. Basch. We wish to express our appreciation to the authorities of the Daresbury Laboratory Synchrotron Radiation Source for allocating beam time and to the staff for their assistance.

[1]G. Bradley Armen *et al.*, Phys. Rev. Lett. **54**, 182 (1985).

[2]H. W. Schnopper, Phys. Rev. **131**, 2558 (1963); R. P. Madden and K. Codling, Phys. Rev. Lett. **10**, 516 (1963); F. Wuilleumier and C. Bonnelle, C. R. Acad. Sci. Ser. B **270**, 1229 (1970).

[3]R. D. Deslattes, R. E. LaVilla, P. L. Cowan, and A. Henins, Phys. Rev. A **27**, 923 (1983).

[4]M. Deutsch and M. Hart, Phys. Rev. A **29**, 2946 (1984), and J. Phys. B **17**, L395 (1984).

[5]S. I. Salem, A. Kumar, K. G. Schiessel, and P. L. Lee, Phys. Rev. A **26**, 3334 (1982); S. I. Salem and A. Kumar, J. Phys. B **19**, 73 (1986), and references therein.

[6]J. P. Desclaux, Comp. Phys. Commun. **9**, 31 (1975).

[7]C. Froese-Fischer, in *Progress in Atomic Spectroscopy, Part C,* edited by H. J. Bayer and H. Kleinpoppen (Plenum, New York, 1984).

[8]M. Breinig, M. H. Chen, G. E. Ice, F. Parente, and B. Crasemann, Phys. Rev. A **22**, 520 (1980); J. A. Bearden, Rev. Mod. Phys. **39**, 78 (1967).

[9]M. Deutsch and M. Hart, J. Phys. B **19**, L303 (1986).

[10]One of these features is visible in Fig. 1 of B. M. Kincaid and P. Eisenberger, Phys. Rev. Lett. **34**, 1361 (1975), but is not mentioned in the text.

[11]C. E. Moore, U. S. National Bureau of Standards Report No. 467, 1949 (unpublished).

[12]J. Reader, J. Opt. Soc. Am. **65**, 286 (1975).

[13]J. Reader and G. L. Epstein, J. Opt. Soc. Am. **62**, 1467 (1972).

[14]M. O. Krause, in *Photoionization and Other Probes of Many-Electron Interactions,* edited by F. J. Wuilleumier (Plenum, New York, 1976).

[15]T. Aberg and G. Howat, in *Handbuch der Physik,* edited by W. Melhorn (Berlin, Springer, 1984), Vol. 31.

[16]J. Tulkki and T. Aberg, J. Phys. B **18**, L489 (1985).

[17]F. Wuilleumier and M. O. Krause, Phys. Rev. A **10**, 242 (1974).

[18]T. A. Carlson, C. W. Nestor, T. C. Tucker, and F. B. Malik, Phys. Rev. **169**, 27 (1968).